Ion Beam Deflection (IBD) Demonstration Mission Concept Study

IEPC-2024-111

Presented at the 38th International Electric Propulsion Conference
P. Baudis Convention Center, Toulouse, France
June 23-28, 2024

John Brophy,[1] Paul Chodas,[2] Steve Chesley,[3] Jon Sims,[4] Shawn Johnson,[5] Reza Karimi,[6] and William Frazier[7]
Jet Propulsion Laboratory/California Institute of Technology,
Pasadena, CA, 91109, USA

Once NASA has completed the Congressionally-mandated task to find at least 90% of the Near-Earth Objects (NEOs) greater than 140 m in diameter, the most likely threat object size for planetary defense will be asteroids in the range 50-140 m dia. The use of a Kinetic Impactor (KI), one of the leading planetary defense techniques, on an asteroid in this size range is likely to disrupt the asteroid if strikes it hard enough to deflect it, with largely unpredictable results. Ion beam deflection (IBD) is a relatively new planetary defense technique in which an ion beam is used to deflect the threat object. The advantages of IBD include: no possibility for disruption, precise deflection control, and the application of the deflection force in the optimal direction. IBD is independent of the composition, strength, spin state, and lighting conditions of the asteroid and only weakly dependent on its shape. Because IBD requires the planetary defense vehicle to rendezvous with the threat object, it provides the opportunity for characterization of the object prior to the start IBD deflection operations. This enables determination of the optimum deflection direction and how long deflection operations will take. Before an actual planetary defense application of IBD is executed, a demonstration of this technique is almost certainly necessary. A demonstration mission would establish the validity of the basic physics, retire known risks, and mitigate unknown unknowns. Specifically, it would demonstrate simultaneous asteroid-relative station keeping, attitude control, and momentum management in the face of gravitational disturbances, solar radiation pressure, thrust and thrust-vector uncertainties, and navigation sensor biases and errors. We identified nine near-Earth asteroids as attractive targets for a potential IBD demonstration mission in the 2030s. We selected one of these, 2004 JN1, and showed that an IBD vehicle with a 2.9-kW (BOL at 1 AU) solar array could rendezvous with, characterize, and produce a measurable deflection of this asteroid in a total mission duration of less than one year.

Nomenclature

a	semi-major axis (AU)
$C3$	hyperbolic excess energy (km^2/s^2)
e	orbit eccentricity
H	absolute magnitude
i	orbit inclination (deg.)
q	perihelion distance (AU)
$Vbar$	asteroid orbital velocity vector (m/s)
α	ion beam divergence half angle (degrees)
ΔV	change in velocity (m/s)

[1] Engineering Fellow, Project Systems Engineering & Formulation, 4800 Oak Grove Drive/301-170S, Pasadena, CA, AIAA Fellow.
[2] Program Area Manager, Mission Systems & Operations, 4800 Oak Grove Drive/301-121, Pasadena, CA.
[3] Navigation Engineer, Solar System Dynamics, 4800 Oak Grove Drive/301-121, Pasadena, CA.
[4] Group Supervisor, Outer Planet Mission Analysis, 4800 Oak Grove Drive/301-121, Pasadena, CA.
[5] Guidance and Control Engineer, Spacecraft Guidance & Control Analysis, 4800 Oak Grove Drive/198-326, Pasadena, CA.
[6] Mission Design Engineer, Outer Planet Mission Analysis, 4800 Oak Grove Drive/301-121, Pasadena, CA.
[7] Group Supervisor, Project Chief Engineering Staff, 4800 Oak Grove Drive/301-170S, Pasadena, CA.

I. Introduction

The objective of this study is to identify the key features of a demonstration mission for the planetary defense technique known as Ion Beam Deflection. The study identifies the major technology issues for IBD that can only be fully mitigated through a demonstration mission.

In 2021, the Planetary Defense Missions, Rapid Mission Architecture Study [1] concluded that, "The results, across a sampling of 15 impacting asteroid trajectories, indicate not only that KI and IBD have similar overall performance envelopes, but also that the risk of asteroid disruption is a significant limitation for successful KI deflections over a large region of the parameter space." This is supported by modeling of the surface strength of the asteroid Bennu [2] which suggests that it could be extremely weak, of order 2 Pa. The gentle, but steady push provided by IBD, however, contains no risk of disruption even for such very weak rubble pile asteroids. For example, a full-scale IBP system providing a force of 500 mN on a 50-m diameter asteroid would create a pressure of roughly 2.5×10^{-4} Pa, orders of magnitude too low to disrupt the asteroid. However, a force of 500 mN on a 50-m diameter asteroid could produce a measurable deflection in a couple of days and provide a ΔV to the asteroid of 1 cm/s in approximately one month (assuming an asteroid density of 1.6 g/cm^3).

In 2005, Congress passed the George E. Brown Jr. Near-Earth Object Survey Act that directs NASA to discover at least 90% of the Near-Earth Object (NEO) population greater than 140 m in diameter. Once this survey is complete and assuming no asteroids are found that are on a collision course with Earth, then the major threat from near-Earth objects becomes those in the size range roughly 50-m to 140-m diameter [2]. Asteroids less than 50-m diameter, while numerous, are generally considered too small to warrant deflection. This can be seen in the chart from [1] reproduced here as **Fig. 1**. This chart indicates that Civil Defense is the most likely response for dealing with asteroids less than 50 m in diameter. **Figure 1** also indicates that IBD is a leading candidate to deflect objects in this size range (50 m to 140 m diameter) since both kinetic impactors (KI) and nuclear deflection would both most likely disrupt such objects.

II. IBD Characteristics

The basic configuration for an IBD system is shown in **Fig. 2**. IBD works by directing a beam of high-energy ions into the surface of the threat object transferring the momentum of the ions to the object through inelastic collisions [3-5]. This is conceptually similar to a kinetic impactor with the impinging ions taking the place of the impacting spacecraft, but with two important differences. First, an IBD system can be designed so that the ions impact the asteroid surface at speeds much greater than is practical for kinetic impactors and in the direction most effective for deflection. Ion impact speeds of 70 km/s are readily achievable, which would be roughly four to five times the impact speed of a kinetic impactor spacecraft. Second, finite power levels for the IBD vehicle means the transfer of momentum is necessarily spread out over time, typically over a timescale of months to years.

Figure 2 also illustrates another important feature of IBD which is the need to thrust nearly equally in opposing directions. The ion beam directed at the asteroid provides the coupling force between the IBD spacecraft and the asteroid. The ion beam directed away from the asteroid maintains the spacecraft-to-asteroid separation distance during IBD operations. It is this ion beam that effectively pushes the spacecraft-asteroid system.

A. Key Features

Reference 1 says, "the efficacy of kinetic impactors and nuclear deflection planetary defense deflection methods depends on the mass, cohesiveness, and other physical properties of the object." Significantly, IBD systems are independent of many key asteroid characteristics including cohesiveness, rotation state, and composition. They are only weakly dependent on the shape of the asteroid, where the efficiency may be lower for less spherically-shaped objects since this could result in a larger fraction of ions missing the asteroid. Like all planetary defense techniques, IBD effectiveness is highly dependent on the asteroid mass.

Ion beam deflection provides fine control of the asteroid trajectory modification and even though it is a "slow-push" planetary defense technique, it provides significantly higher forces than other slow-push technologies such as a "gravity tractor." It also enables a much larger standoff distance than a gravity tractor which increases spacecraft safety and simplifies fault management. Importantly, the amount of force that can be applied by an IBD system is completely under the control of the IBD system engineering. It does not depend on the characteristics of the threat object.

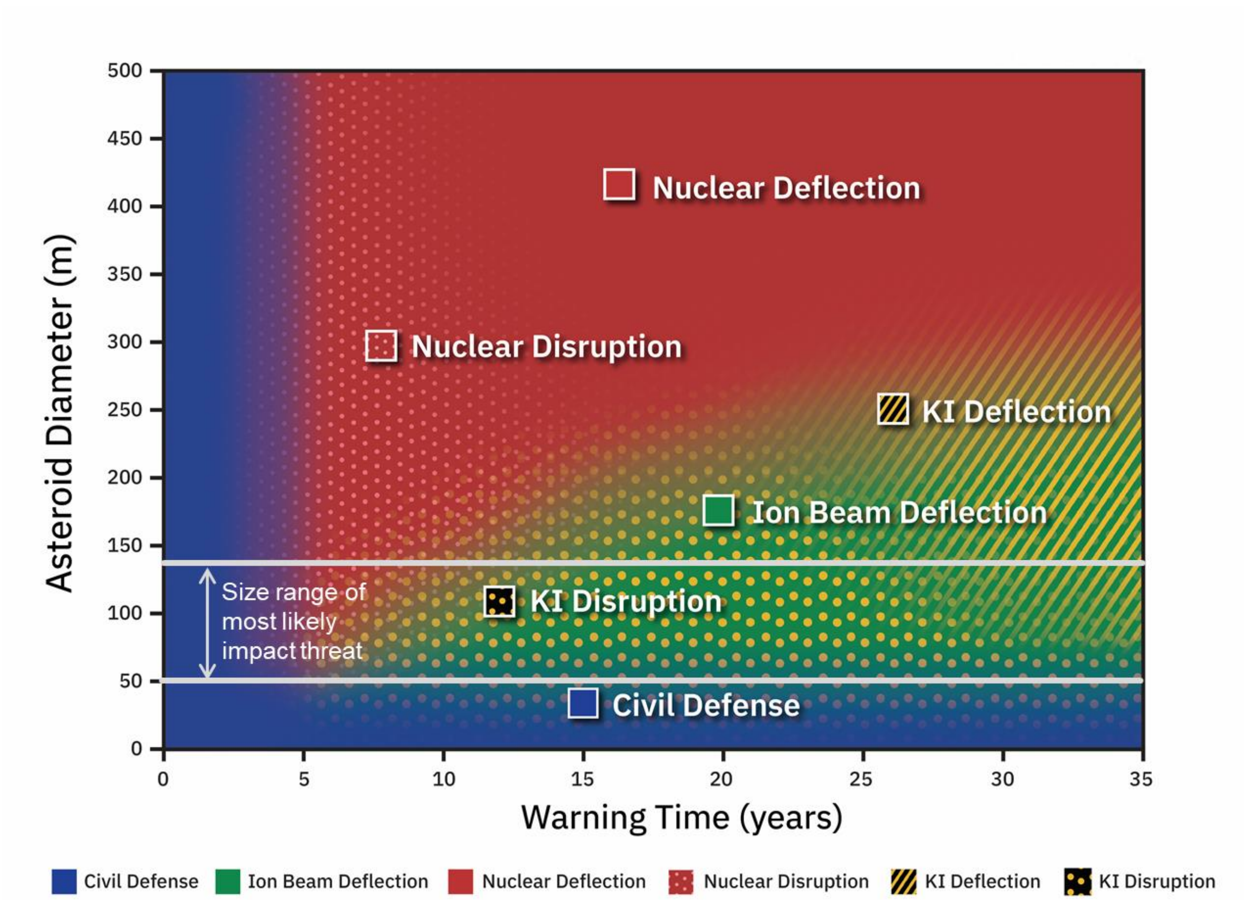

Figure 1. Summary of deflection capabilities from [1]. The two horizontal light gray lines (not original to the figure) are added to indicate the range in asteroid diameter that represent the most likely impact threat. It is clear from this graphic that IBD is a potentially attractive planetary defense technique for this size range.

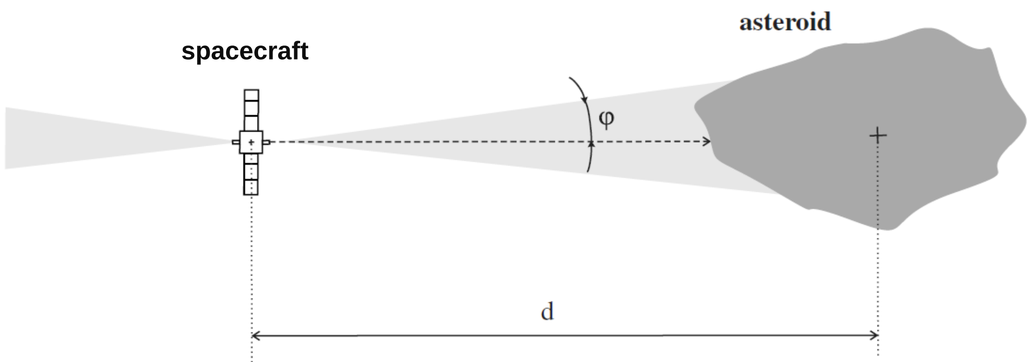

Figure 2. Basic ion beam deflection configuration (from Ref. 2).

IBD requires rendezvous with the threat object. Consequently, it naturally enables detailed characterization of the asteroid's mass, shape, and orbit prior to deflection operations. It enables determination whether deflection is actually required and, if so, the direction which minimizes the required deflection ΔV. The detailed characterization also enables an accurate determination of how long the deflection will take.

B. Key Requirements

The key requirements of an IBD system for planetary defense include:

- Rendezvous with the threat object. If the IBD deflection system can also be used for electric propulsion transfer to the asteroid, then no additional propulsion system for trajectory modification is required.
- Station keeping with the asteroid. It is necessary for the IBD vehicle to remain at a selected distance from the c.g. of the asteroid during deflection operations for months or years at a time.
- Thrust along the asteroid's velocity vector. This is generally the most efficient direction. An IBD System must be capable of thrusting either in the direction of motion or against it, whichever is better for the particular threat object.
- Provide detailed characterization of the asteroid's mass, shape, and orbit prior to deflection operations. This will provide accurate knowledge of how long the deflection will take and in which direction the asteroid should be deflected.
- Control the attitude and momentum of the IBD vehicle during IBD operations for months at a time.
- Have a fault protection approach that protects the IBD vehicle in the event of spacecraft faults.
- Provide the capability for continuous telecom capability with Earth during deflection operations.

C. Loss Mechanisms

There are two primary loss mechanisms for IBD systems: ions directed toward the asteroid that miss; and gravitational losses. Both of the loss mechanisms are strongly affected by the standoff distance, *d*, between the spacecraft and the asteroid. To minimize the fraction of ions that miss the asteroid, the separation distance should be minimized. To minimize the gravitational losses, the separation distance should be maximized. The tradeoff between these competing effects determines the desired IBD-to-asteroid distance during deflection operations.

The gravitational force between the spacecraft and the asteroid is shown in **Fig. 3** as a function of standoff distance for 50-m diameter and 140-m diameter asteroids (assuming an asteroid density of 2 g/cm^3). At five asteroid diameters to the surface for a 140-m diameter asteroid, the gravitational force is $3\text{x}10^{-7}$ N per kilogram of spacecraft mass. For a 3000-kg spacecraft, this is a force of about 1 mN, which is just 0.2% of a hypothetical IBD system that provides a force of 500 mN. This example indicates that a standoff distance of around five asteroid diameters is sufficient to reduce gravitational losses to less than 1%.

The maximum standoff distance that an IBD system can have and still result in 90% of the ion beams impacting the asteroid (assuming a spherical asteroid) is given in **Fig. 4** for an ion beam divergence half angle, α, of 5 degrees. This figure indicates that a standoff distance of five times the asteroid diameter is achievable with a five-degree beam divergence half angle.

The ion optics computer code CEX2D [6] was used to determine if a beam divergence half angle of 5 degrees is achievable. This code was used to simulate the ion beam divergence angles of dozens of candidate ion optics designs. The six best cases are given in **Fig. 5** which shows the beam divergence half angle as a function of the fraction of maximum extractable ion beam current through each grid aperture, J/J_{max}. The solid green line indicates a half angle of 5 degrees. This figure indicates that beam divergence half angles of less than or equal to 5 degrees can be obtained over ratios of J/J_{max} from 0.45 to 0.80. This is a sufficiently large range that is consistent with the plasma density variation across the grids of modern ion thrusters. Consequently, the low-beam-divergence ion optics from **Fig. 5** could be successfully installed and operated on existing ion engines, such as NEXT [7] or NEXIS [8].

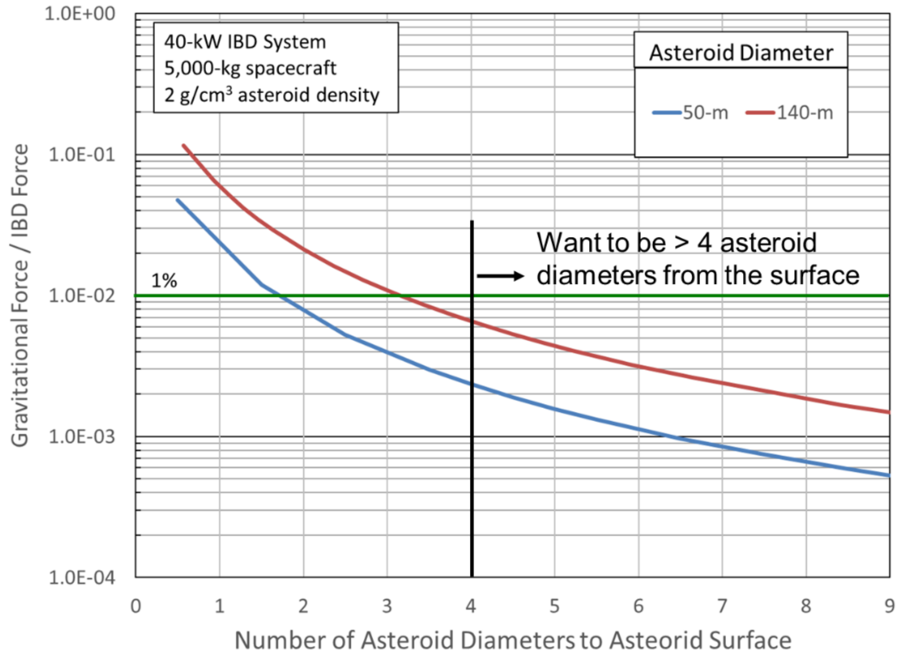

Figure 3. The gravitational force per kilogram of spacecraft mass, assuming an asteroid density of 2 g/cm^3, over the size range corresponding to the most likely impact threat decreases to a negligible value for standoff distances greater than roughly four asteroid diameters.

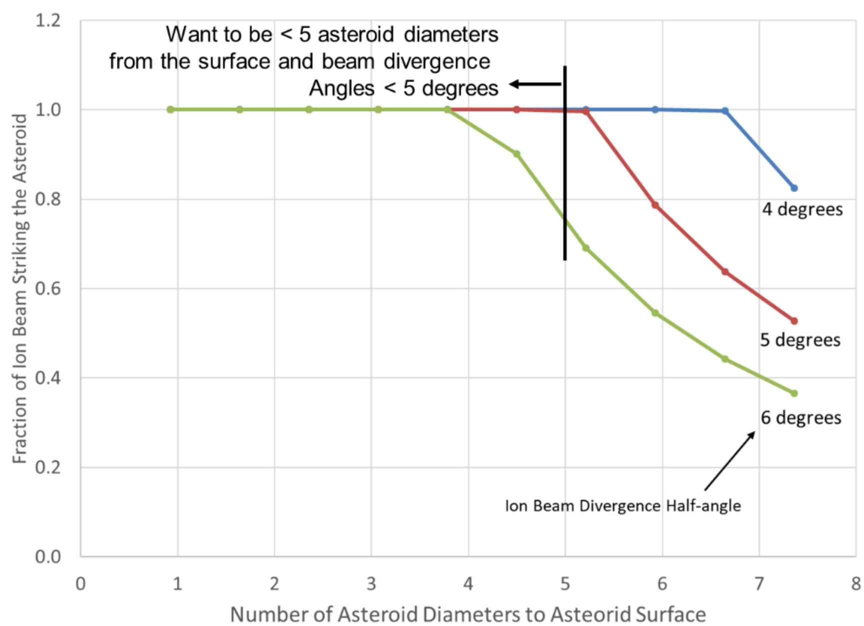

Figure 4. The maximum surface standoff distance for which ~90% of the ion beam impacts a spherical asteroid is approximately five times the asteroid diameter for a beam divergence half angle of α = 5 degrees.

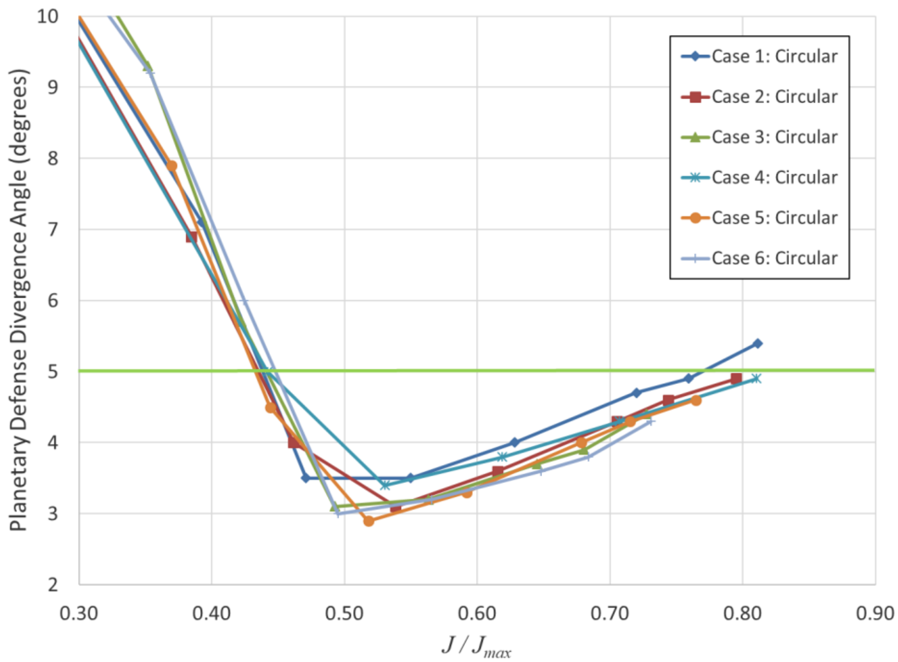

Figure 5. Simulated ion beam divergence half-angles that encompass 90% of the beam ions are calculated using the CEX2D computer code. These results indicate that beam divergence half-angles of less than ~ 5 degrees are achievable over a sufficiently large range of beam current ratios to be practical. The different cases indicated correspond to different grid geometries with circular apertures and flat grids.

III. IBD Demonstration Mission

While the concept for ion beam deflection of potentially hazardous asteroids has been around for over a decade [9], it has not been examined extensively by the planetary defense community. Consequently, there are important unresolved feasibility issues. It is likely that satisfactory resolution of these issues can only be done through a demonstration mission.

A. Key Feasibility Issues

The following four key feasibility issues have been identified for IBD:

1. Does the physics of IBD work as claimed? That is, does the impinging ion beam successfully transfer all of its momentum to the object it strikes?
2. Can the IBD spacecraft adequately perform station keeping with the asteroid during extended IBD operations?
3. Can the attitude and momentum of the IBD spacecraft be adequately controlled during extended IBD operations?
4. Can an IBD system be designed that is robust to the uncertainties of important target characteristics including: mass, size, shape, strength, spin rate, and spin pole orientation?

While it is likely that each of the above issues could be adequately resolved through analysis and testing on the ground, it is unlikely that this would be sufficient to convince a skeptical community that all of the unknown unknowns have been sufficiently mitigated. The situation is similar to the first use of solar electric propulsion (SEP) in deep space prior to the flight of Deep Space 1 (DS1) in 1997. DS1 proved the utility and operability of SEP in a way that no ground test could leading directly to its spectacular use on NASA's Dawn mission. This utility of a demonstration mission is especially true for IBD where its functionality must be guaranteed if it is to be relied on to deflect a hazardous object on an impact trajectory with Earth.

B. Objectives of an IBD Demo Mission

To address the four key feasibility issues above, the following major objectives of an IBD demonstration mission must be met:

1. Rendezvous with a near-Earth asteroid not previously visited by a spacecraft.

2. Perform pre-IBD-deflection-characterization including: determination of the asteroid mass and generation of a shape model.
3. Demonstrate station keeping during IBD operation.
4. Demonstrate spacecraft attitude control during IBD operation.
5. Demonstrate momentum management during IBD operation.
6. Perform Verification and Validation of fault management applicable to IBD operation.
7. Demonstrate weeks to months of IBD operation.
8. Create a measurable deflection of the asteroid.
9. Demonstrate that the measured deflection agrees with the predicted deflection within the uncertainties.

IV. Candidate Asteroids for a Demonstration Mission

We did a search to find near-Earth asteroids that could be suitable candidates for a demonstration mission in the 2030's. The search was limited to asteroids with absolute magnitudes, H, in the range $24.2 \geq H \geq 23.7$ corresponding to diameters of roughly 50 m. Since the albedos of these asteroids are unknown, the actual size is a function both of the observed absolute magnitude H and the albedo as indicated in **Table 1** which covers a reasonable range of albedos for near-Earth asteroids. We focused our attention on roughly 50-m diameter asteroids since this is at the low end of the size range for threat objects of interest, which would make the demonstration mission easier, but not so small that the demonstration could be dismissed as an irrelevant stunt.

Table 1. Asteroid diameter in meters.

H	Albedo				
	0.05	**0.14**	**0.18**	**0.20**	**0.25**
24.2	86	47	45	43	38
24.1	90	54	47	45	40
24.0	94	56	50	47	42
23.9	99	59	52	49	44
23.8	103	62	54	52	46
23.7	108	65	57	54	49

In addition to size, we looked for asteroids for which there are launch dates in the 2030's; that have well known orbits (Orbit Condition Code ≤ 1); that have a Minimum Orbital Intersection Distance (MOID) > 0.015 au; that don't get too close to the Sun (perihelion distance q > 0.85 au); and that have accessible orbits. The perihelion constraint (< 0.85 au) is included for thermal reasons to minimize the challenges of designing a spacecraft that has to go inbound toward the Sun as well as outbound. The MOID constraint is to reassure everyone that the demonstration deflection will not create an impactor! Candidate asteroids must not be on the Sentry risk list [10]. Finally, we looked for asteroids that are relatively easy to rendezvous with. The resulting list is given in **Table 2**.

Table 2. List of Candidate Asteroids for an IBD Demonstration Mission.

Target Asteroid	*H*	*a* (*AU*)	*e*	*i* (*deg*)	*q* (*AU*)	MOID (AU)	Launch Date	*C3* (km^2/s^2)	TOF (years)	Xenon (kg)
2019 JU5	24.0	1.0723	0.1927	2.57	0.8656	0.0236	4/16/29	12.4	0.46	68
2004 JN1	23.7	1.8053	0.1757	1.50	0.8947	0.0234	3/5/30	3.8	0.78	40
2015 MB54	24.1	1.2098	0.2403	2.75	0.9950	0.0234	3/29/30	11.5	0.45	66
2001 KM20	23.9	1.1838	0.2091	3.73	0.9362	0.0162	5/29/32	23.1	2.8	50
2012 BA35	23.8	1.0707	0.1159	5.81	0.9466	0.0179	8/24/32	6.5	0.95	136
2013 VM13	24.2	1.2023	0.0364	3.22	1.1586	0.1823	11/4/32	4.4	3.0	84
2012 GA5	24.2	1.1420	0.664	7.30	1.0662	0.0971	10/15/33	10	1.7	156
2005 FG	23.9	1.1210	0.2126	3.90	0.8827	0.0161	8/21/37	10	0.48	71
2007 HL4	24.1	1.1200	0.0907	6.54	1.1085	0.0314	4/22/38	13.9	1.7	35

For each of the asteroids in **Table 2**, low-thrust rendezvous trajectories were generated assuming the use of a Falcon 9 Recoverable launch vehicle, a 2.9-kW (BOL at 1 AU) solar array and an electric propulsion (EP) subsystem using Halo 12 Hall thrusters [11]. The spacecraft (non-EP) power consumption was assumed to be 250 W with a dry mass of 1000 kg. A maximum of two Hall thrusters were operated at a time and a maximum EP duty cycle of 85% was assumed (which is consistent with JPL's practice for early formulation mission design with

SEP). The resulting launch dates, launch *C3*, time-of-flight (TOF) and xenon required for rendezvous are given in the last four columns of **Table 2**. The nine asteroids identified in **Table 2** are sorted by launch date. The launch dates range from 4/16/2029 through 4/22/2038, providing substantial programmatic flexibility since any one of the asteroids in this table would be a good target for an IBD demonstration mission.

V. Demonstration Mission Point Design—Concept of Operations

We selected one asteroid from **Table 2**, 2004 JN1, to use as an example for an IBD demonstration mission. This asteroid is on the bigger side of the candidate asteroids in **Table 2** and has a good launch opportunity in 2030. An example trajectory to 2004 JN1 is given in **Fig. 6** for a 3/5/2030 launch. The time-of-flight to rendezvous with the asteroid is just under half a year and requires a modest 68 kg of xenon propellant. Because we are assuming the use of SEP to perform the rendezvous, there are actually multiple launch opportunities in the 2030's to 2004 JN1 as indicated in **Fig. 7**. This figure shows launch opportunities in 2029, 2030, 2031, 2038, and 2039.

A. Approach and Characterization

For the example trajectory in **Fig. 6**, the IBD spacecraft arrives at 2004 JN1 in October 2030. We assume three months for characterization of the asteroid followed by a slow descent to the operational altitude. IBD deflection operations begin in Jan 2031 (90 days post-rendezvous) and continue for 30 days. A hydrazine reaction control subsystem (RCS) is used to maneuver in proximity of the asteroid to perform reconnaissance maneuvers enabling rapid characterization of the asteroid. The characterization phase includes multiple flybys of around 10-km altitude to map the asteroid to enable shape modeling and limb modeling to a resolution required for subsequent IBD operations. Sub-kilometer altitude flybys are used to obtain the asteroid mass as was done in the OSIRIS-REx mission where three slow-speed flybys reduced the mass uncertainty of the asteroid Bennu to 1%.

At the end of the characterization phase, the proximity operations transition to that shown in **Fig. 8**. The spacecraft uses the RCS for a dog-leg maneuver to shift from a range of 2-3 km altitude to 1-2 km. The resulting station-keeping checkout position along the asteroid's velocity vector, *Vbar*, is used to demonstrate the capability of the relative navigation and station-keeping control while starting the initial deflection of the asteroid with only partial ion beam momentum exchange. Once demonstrated at the high-altitude, the spacecraft will descend to a lower set point altitude where a staged approach to demonstrating the safety of the deflection will occur. Finally, the spacecraft will enter its nominal station-keeping altitude, where it will remain for the remainder of the deflection operations.

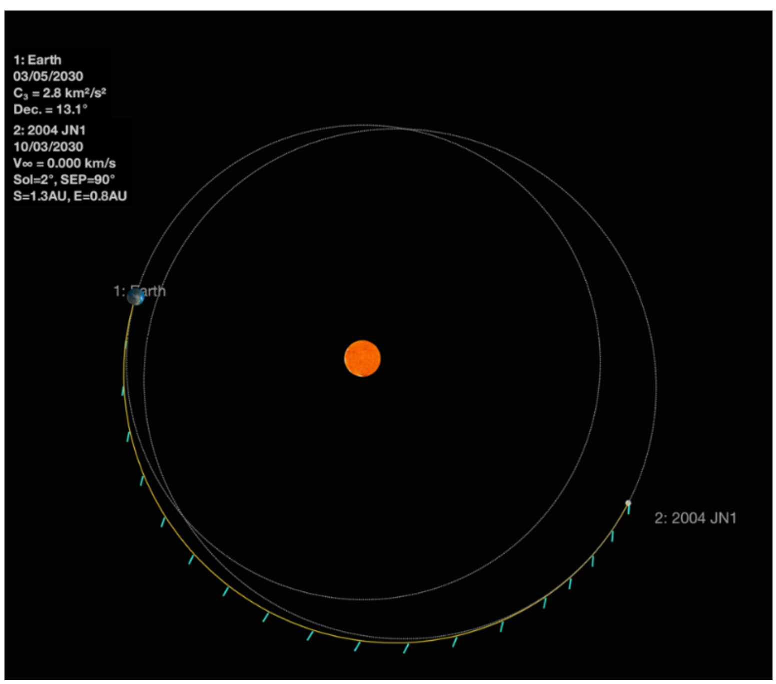

Figure 6. Example low-thrust rendezvous trajectory to asteroid 2004 JN1.

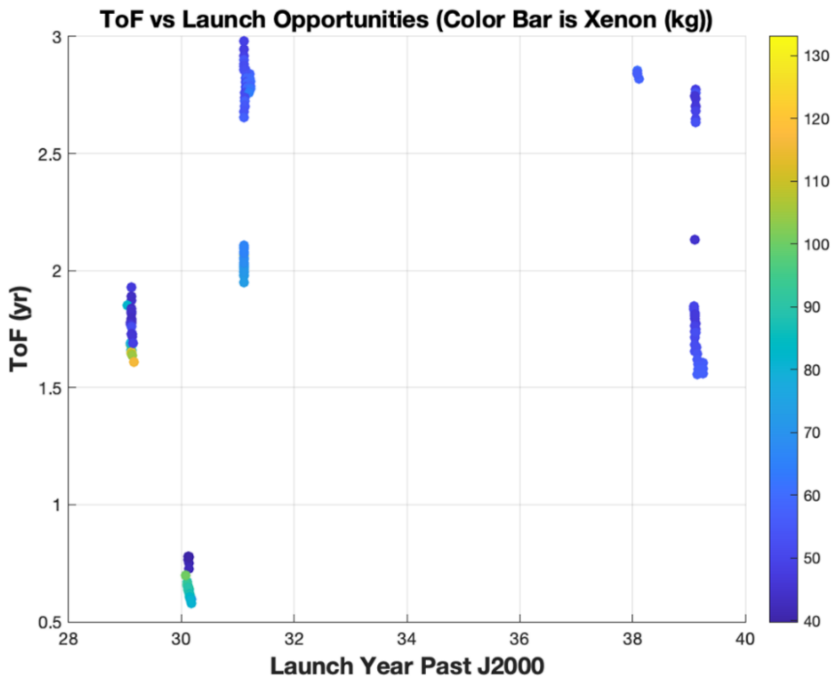

Figure 7. There are multiple launch opportunities for low-thrust rendezvous trajectories to 2004 JN1.

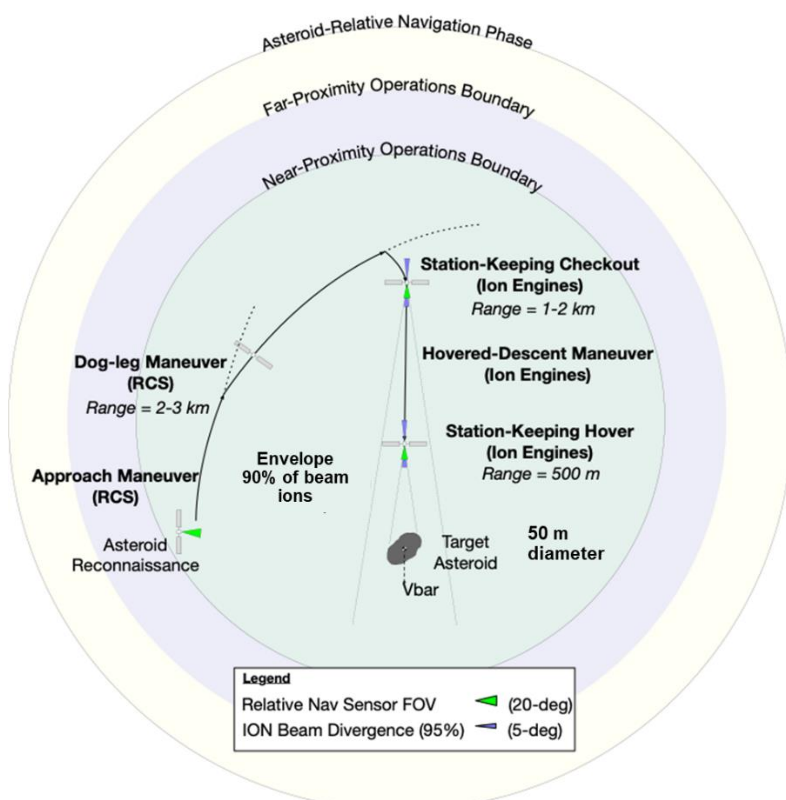

Figure 8. Preliminary approach and proximity concept of operations.

B. Guidance, Navigation and Control (GNC)

Guidance, navigation, and control for an asteroid deflection demonstration must respond to the challenge that a real deflection mission will have to function at a target asteroid whose characteristics are uncertain at the time the IBD spacecraft and mission operations are designed. This motivates a design that is robust to large uncertainties in important characteristics such as albedo, size and shape, angular momentum vector (spin state), and illumination geometry. Further, the GNC subsystem must be capable of operating continuously for long durations, on the order of months or years, to be effective.

An asteroid deflection mission using IBD must be highly reliable, which emphasizes the use of existing, flight-proven technologies to the maximum extent possible along with the execution of a realistic demonstration mission to mature elements of the GNC design that lack heritage. In order to identify the existing GNC challenges, a survey of GNC hardware and algorithms from previous asteroid missions, with a focus on extensibility to an ion-beam deflection mission, is summarized in **Table 3**.

Heritage spacecraft GNC hardware are leveraged in this IBD demonstration mission concept, including star trackers, inertial measurement units (IMUs), and Sun sensors for attitude knowledge. SEP cruise is assumed to occur on a pair of the gimbaled ion engines. A set of redundant reaction wheels is assumed as the primary attitude control actuator to provide stable pointing and fuel-efficient attitude/momentum management via the gimbaled ion engines. The RCS is used as a backup attitude control system for the RWAs, asteroid proximity maneuvers, and for the execution of certain key safe modes.

Station-keeping in close-proximity to an asteroid drives the need for a highly reliable sensor suite that can successfully operate over a large uncertainty in lighting conditions. The two sensing solutions that have been employed in previous missions are LIDAR-based measurements and Imager-based measurements and most spacecraft have flown both (**Table 3**). LIDAR provides a versatile sensor that can be operated in both range-finding and imaging modes. The laser power of the LIDAR is selected to accommodate large uncertainty in asteroid albedo and to operate over a large variation in altitudes from 100s of meters to several kilometers. This is necessary to ensure spacecraft safety during IBD operations. A LIDAR in imaging mode provides a measured center-of-geometry of the asteroid along with the measured range that can be used as a reference signal for control.

If sufficient time is allocated in the mission plan for a detailed mapping phase, an imaging LIDAR could be used to perform terrain-relative navigation with feature detection to better manage possible oscillatory range measurements as a function of non-spherical shape and spin state. Alternatively, a fixed range could be considered if ion engine throttle and control authority are compatible with the asteroid shape and spin state. There is a trade space to consider in terms of algorithm complexity, asteroid physical properties uncertainty, mission responsivity, and risk tolerance. Future studies should investigate how best to design a navigation system that is robust across a large variability in target physical properties (e.g., size, shape, and albedo). Most likely this will require consideration of a multi-pronged approach to navigation with overlapping redundant capabilities in sensors to ensure navigation measurements are available and sufficiently fault-tolerant to perform the station-keeping maneuver with very high reliability.

The guidance strategy proposed for our demonstration mission leans on heritage to deliver the spacecraft to the local proximity of the asteroid, where navigation transitions to an asteroid-relative phase via an optical navigation approach. From there, the short characterization phase is expedited via LIDAR measurements to eliminate the time necessary to execute a Statistical Process Control (SPC)-based characterization phase with multiple phase angles. After the expedited characterization, a ground-planned RCS maneuver is utilized to deliver the spacecraft to a safe home-base along the *Vbar* of the asteroid and constrained to put the nominal thrust direction of the ion engines directed along the *Vbar* and in the direction of the asteroid center at a distance of several kilometers, but within the dynamic range of the LIDAR used in a range mode with enough signal-to-noise to suitably maintain regular-cadence direct range measurements to the asteroid surface. The system is designed to permit a power-positive and telecom safe orientation in this deflection geometry. From there, the planned path is to remain on the *Vbar* at a fixed distance from the visible center of geometry of the asteroid as detected by the imaging LIDAR. A wide-angle camera is also employed as a redundant measurement and designed to be consistent with the asteroid type and expected illumination.

Table 3. GN&C Heritage from Previous Missions to Near-Earth Asteroids.

<table>
<tr><th colspan="2"></th><th>OSIRIS-REx</th><th>Hayabusa</th><th>Hayabusa2</th><th>NEAR</th><th>DART</th></tr>
<tr><th colspan="2">Asteroid</th><td>Bennu</td><td>Itokawa</td><td>Ryugu</td><td>Eros</td><td>Didymos I (Dimorphos)</td></tr>
<tr><th colspan="2">Albedo</th><td>0.044 ± 0.002 (visible, global average) [12]</td><td>0.53 ± 0.04 (visible) [13]</td><td>0.045 ± 0.002 (visible) [14]</td><td>0.25 ± 0.06 (visible) [15]</td><td>0.15 ± 0.02 (visible) [16]</td></tr>
<tr><th colspan="2">Extent</th><td>Ellipsoidal radii:
X: 252.37±0.09 m
Y: 245.91 ± 0.09 m
Z: 228.37 ± 0.09 m [17]</td><td>Diameter:
X: 535 ± 1 m
Y: 294 ± 1 m
Z: 209 ± 1 m [18]</td><td>equatorial radius of 502 ± 2 m and polar-to–equatorial axis ratio of 0.872 ± 0.007 [19]</td><td>Ellipsoidal radii:
X: 34.4 ± 0.2 km
Y: 11.2 ± 0.2 km
Z: 11.2 ± 0.2 km [15]</td><td>Ellipsoidal radii:
X: 177 ± 2 m
Y: 174 ± 4 m
Z: 116 ± 2 m [16]</td></tr>
<tr><th rowspan="3">Deep-Space GNC</th><th>Attitude Actuator</th><td>RWAs with RCS desat [20]</td><td colspan="2">RWAs</td><td>RWAs with RCS desat [21]</td><td>RCS</td></tr>
<tr><th>Attitude Sensors</th><td>Star tracker + IMU + Sun sensors [20]</td><td colspan="2">Star tracker + IMU + Sun sensors</td><td>Star tracker + IMU + Sun sensors [21]</td><td>Star tracker + IMU + Sun sensors [22]</td></tr>
<tr><th>Trajectory cntrl actuators</th><td>Hydrazine mono-prop.</td><td colspan="2">4 Ion engines Cruise + RCS for TCMs</td><td>Hydrazine mono-prop</td><td>RCS for TCMs [22]</td></tr>
<tr><th rowspan="10">Prox-Ops GNC</th><th>Proximity Nav Algorithm (Far)</th><td>OLA LIDAR + MAPCAM (for shape/feature models)</td><td colspan="2">Ground ONC-W1-based algorithm (feature/shape matching)</td><td rowspan="3">Ground MSI + NLR (feature/shape model) [23]</td><td rowspan="3">OpNav with DRACO camera Autonav with closure on image centroid [22]</td></tr>
<tr><th rowspan="2">Proximity Nav Algorithm (Near)</th><td rowspan="2">TAGCAMS NFT + GNC LIDAR</td><td colspan="2">LIDAR/LRF-S1 based</td></tr>
<tr><td colspan="2">Onboard TM-Relative: ONC-W1 + FLASH</td></tr>
<tr><th>Proximity attitude guidance</th><td>Inertial-fixed [39]</td><td colspan="2">Inertial attitude target</td><td>Inertial attitude target [24]</td><td>Inertial attitude target [22]</td></tr>
<tr><th>Proximity translational actuator</th><td rowspan="2">0.08-N engine for checkpoint/matchpoint TCM (also had ability to abort)</td><td colspan="2" rowspan="3">RCS [25]</td><td rowspan="4">RCS [24]</td><td rowspan="4">RCS [22]</td></tr>
<tr><th>Descent translational actuator</th></tr>
<tr><th>Descent attitude actuator</th><td rowspan="2">RWAs [20]</td></tr>
<tr><th>Proximity attitude actuator</th><td colspan="2">RWAs [25]</td></tr>
<tr><th rowspan="2">Descent guidance and control</th><td rowspan="2">Polynomial guidance for checkpoint/matchpoint TCMs [20]</td><td colspan="2">On-board PD closure on relay</td><td rowspan="2">Sequential braking TCMs [23]</td><td rowspan="2">Miss-distance correction TCMs (computed autonomously) [22]</td></tr>
<tr><td colspan="2">Ground-based TCM based on opnav</td></tr>
</table>

The RCS subsystem is used for spacecraft safety and for nearby proximity operations to the asteroid where 6-DOF control is required to enter the desired station-keeping asteroid-relative geometry with the spacecraft positioned along the *Vbar* with ion-beam thrust vector centered on the center of geometry of the asteroid. To mitigate navigational uncertainties of the RCS subsystem, coupled engines are required for attitude control. The RCS delivers the flight system to near-proximity range to the asteroid in order to perform a checkout of the relative navigation sensors. The range measurement provided by the sensors is used to improve the orbit determination (OD) of the asteroid. From there, the system is delivered to a "home point" where handoff to the ion-engine station-keeping mode occurs. The home-point is chosen to be a location with sufficient distance where the system is passively safe for several hours to permit onboard autonomy to perform contingency maneuvers. In nominal operations, the ion-engines utilize their throttle capability to lower the spacecraft into the final station-keeping altitude above the asteroid surface for improved deflection efficiency with the ability to raise the system to a higher altitude for checkouts, hardware swaps, or other necessary activities.

In an ion-beam deflection mission, minimizing deflection duration by maximizing linear momentum exchange efficiency with the asteroid is of utmost importance. In this study, angular momentum changes of the asteroid are assumed to be of little consequence. This motivates a strategy that is capable of maintaining all degrees of freedom of control of the spacecraft relative to the asteroid while continuously maintaining ion-beam linear momentum exchange. One of the key features of the ion-beam deflection architecture is that the counter-pointed engines, when coupled with a dual-angle gimbal system, provide the degrees of freedom needed to maintain the deflection, control 3-DOF translation, and provide the capability to dump momentum built up in the reaction wheel assemblies (RWAs). The dual-axis gimbal system is typical for deep space ion engine missions to ensure thrusting through the spacecraft center of gravity (CG). From there, the engines can be configured in such a way that pure translations and pure rotations are possible while maintaining a nominal thrust direction. For example, **Fig. 9** shows a 3-DOF free-body diagram for the two-axis gimbaled two-engine configuration, where T1 and T2 are the thrust vectors of engines 1 and 2, respectively and an arbitrary coordinate system is shown to demonstrate that pure cross-axis forces are achievable while maintaining the deflection. The ion engines can be scaled in number for redundancy and improved efficiency.

For our demonstration mission concept, a 4-engine configuration is assumed, such that only two engines are required to perform the mission objectives, but four ion engines are available to improve the efficiency of the deflection when healthy and also provide redundancy. For any even-engine configuration along with enough gimbal angle range, the IBD spacecraft can be oriented to achieve the deflection direction and also control the planar motion necessary to keep the asteroid centered while maintaining the deflection along the *Vbar*. Reaction wheels are assumed in this architecture to maintain a minimum-phase control system by decoupling the nominal translational and attitude control loops. This has the benefit of improving controller bandwidth.

In this approach, the ion engines are used for momentum management of the reaction wheels while maintaining the ion-beam deflection. This avoids the need to use RCS propellant for this function. However, this choice should be studied further to ensure a controller can be developed with sufficient bandwidth to perform the station-keeping and momentum capability. The RCS system can always be considered for momentum dumping if the design closes for a particular target.

The RCS subsystem serves as an abort mechanism in case any issues arise with the ion engine control or relative navigation sensing. Asteroid deflection is most efficient when thrusting along *Vbar* even for fairly elliptic asteroid orbits. Therefore, one can always assume a Sun- or Anti-Sun pointed maneuver is possible, even when relative navigation is lost. Further, this type of abort can even be performed without inertial attitude knowledge and only Sun sensors and an IMU are necessary. This provides a robust mechanism for fault tolerance when in proximity to the asteroid.

During the station-keeping deflection operations, momentum will accumulate in the reaction wheels due to ion-engine induced roll torques, solar radiation pressure torque, and possibly gravity gradient effects from the asteroid-spacecraft local gravitational attraction. To mitigate roll-torque (e.g., swirl torque) momentum accumulation, the engines will be configured to counter the opposing engine's roll torque, leaving only very small residuals that are managed by the momentum dumping of the wheels.

C. Creating a measurable deflection

The intrinsic brightness of our target asteroid 2004 JN1 is given by its absolute magnitude H = 23.74 mag, which provides only a rough indication of the size and mass because the albedo is unknown. Based on known properties of asteroids, an albedo of 14% is considered a nominal value, with a maximum value of approximately 30% and a minimum value of 3%. This yields a large distribution in potential mass and corresponding acceleration for a given applied force as shown in **Table 4** (assuming a bulk density of 1.6 g/cm^3).

To obtain a measurable deflection, the relative uncertainty of the heliocentric velocity vector is the key. We assume a single pseudo-range measurement with uncertainty of 4 m (0.03 μs) every 10 days after rendezvous (this is twice the error demonstrated by OSIRIS-REx at Bennu) [30]. The goal is to drive the uncertainty an order of magnitude below the expected deflection. When enough time has passed that the uncertainty in the estimated IBD acceleration based on radio tracking drops below the expected accelerations in the third row of **Table 4**, then we have an observable performance that is quantifiable and constitutes a successful demonstration.

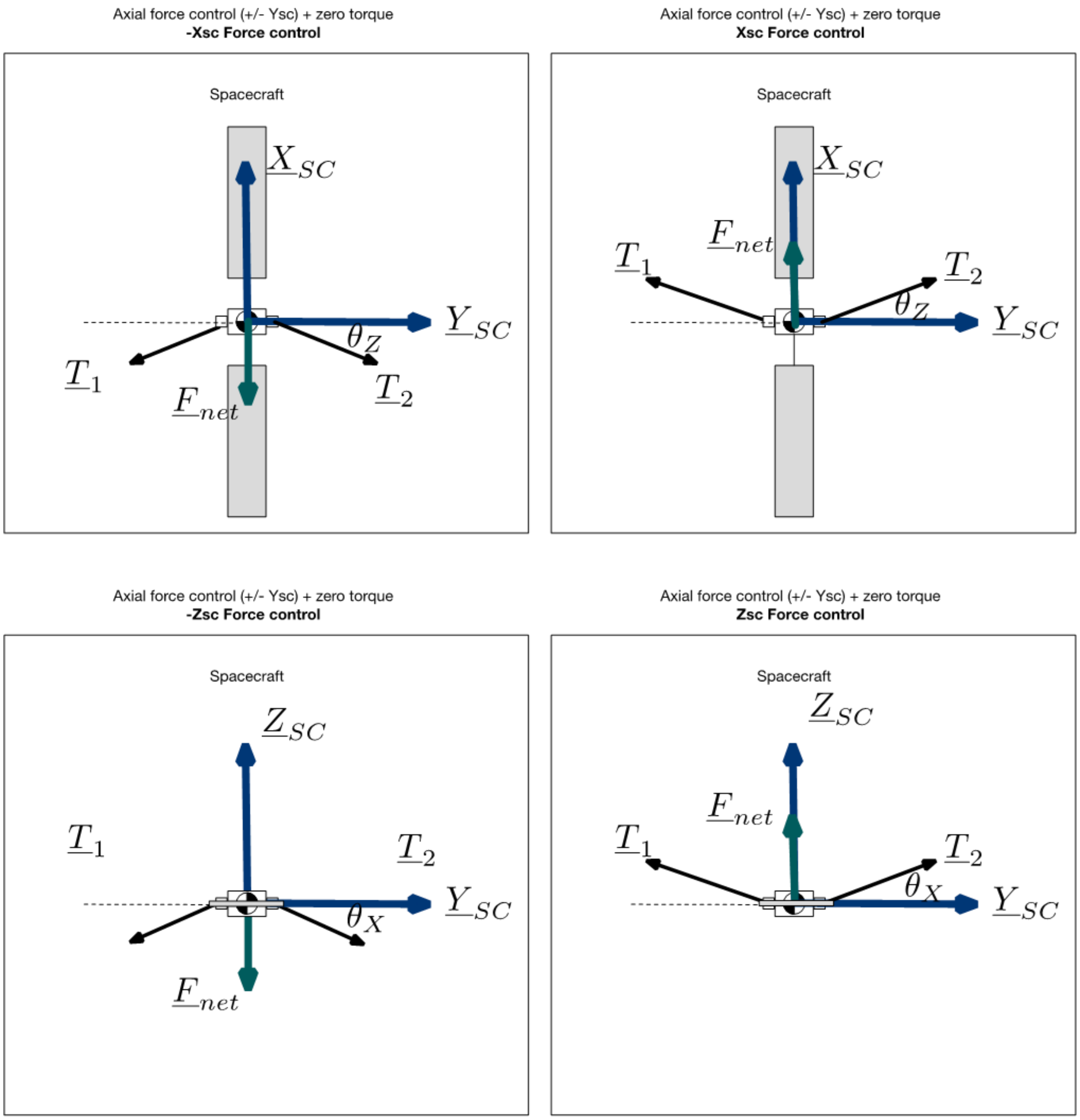

Figure 9. 3-DOF control using single-thruster pair.

Table 4. Deflection of 2004 JN1 over the range of likely albedos for an applied force of 41 mN assuming a density of 1.6 g/cm^3.

	Maximum Albedo	Nominal Albedo	Minimum Albedo
Albedo (%)	30	14	3
Diameter (m)	43	63	137
Mass (kg)	6.8E+07	2.1E+08	2.2E+09
Acceleration (mm/s)	6.0E-07	1.9E-07	1.9E-08
ΔV (mm/s) after 30 days	1.6	0.5	0.05

In this demonstration mission concept, we are assuming a total of 30 days of IBD operation with a force applied to the asteroid of 41 mN. Furthermore, we assume that only 50% of the beam ions strike the asteroid. In an actual operational IBD system using gridded ion thrusters with an ion beam divergence half angle of 5 degrees or less, we would expect that 90% of the beam ions hit the asteroid. In this demonstration mission, however, we are assuming the use of the Halo 12 Hall thrusters due to their low cost even though these thrusters have a significantly larger beam divergence angle. With the assumption that 50% of the ions hit the asteroid, each thruster (the asteroid facing thruster and the opposing thruster) must operate at a thrust level of ~82 mN. For the Halo 12 thruster this requires an input power of 1600 W per thruster at a specific impulse of 1900 s corresponding to a mass flow rate of 4.3×10^{-6} kg/s. Thrusting for 30 days at this thrust level with two thrusters consumes 11 kg of xenon. We add this to the 68 kg required to rendezvous with the 2004 JN1 to get a total xenon requirement of 79 kg. This is well within the propellent throughput capability of the Halo 12 thrusters.

The observable acceleration of the target body is small as indicated in **Table 4** because it is effectively being tracked indirectly by virtue of the spacecraft optical navigation and radio tracking. This error is initially on the order of 10^{-7} mm/s^2 but then is reduced by more than an order of magnitude as additional tracking data are gathered during the encounter (**Fig. 10**). For the bright (30%) and moderate albedo (14%) cases, the target acceleration is observable before end of thrusting because the 3-sigma uncertainty in the estimated IBD acceleration is less than the expected IBD acceleration shown by the top two horizontal lines (taken from the 4th row in **Table 4**). For the dark, minimum albedo (large) object case, deflection is confirmed with ~6-sigma confidence ~30 days after thrusting concludes, even though the achieved ΔV here is small, only 0.05 mm/s. Therefore, this demonstration is robust to a reasonable range of target albedos, which corresponds to a factor of 32 variation in mass (third row in **Table 4**).

However, this doesn't tell the whole story since the data in **Table 4** are for one particular asteroid density of 1.6 g/cm^3. While this is a reasonable value, it obviously doesn't cover the range of possible asteroid densities which could be from 1 to 6 g/cm^3 or more. For example, asteroid Bennu has a density of 1.26 g/cm^3, Apophis 2.6 g/cm^3 and stony-iron asteroids up to about 6 g/cm^3. Iron asteroids could have densities approaching 8 g/cm^3. Increasing the mass variation to account for a factor of six or more in density variation in the values in **Table 4** would greatly complicate an IBD demonstration mission. Consequently, a more likely approach, and the one recommended in this paper, is that any target for an IBD demonstration mission must have near-IR observations such as provided by NEO Surveyor. Such observations would reduce the mean diameter uncertainty from a factor of 3 to about 25% and reduce the mass uncertainty at a fixed density by an order of magnitude from a factor 32 to a factor of 3. Adding in the effect of a possible factor of 6 variation in density would result in a factor 18 variation in mass for asteroids with near-IR observations. This is large, but still significantly less than the range given in **Table 4**.

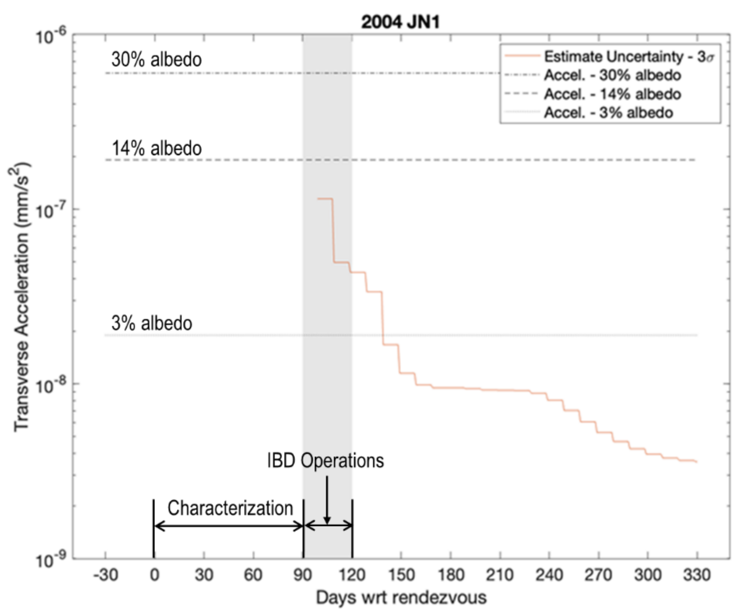

Figure 10. An observable acceleration due to IBD operation is possible in less than 150 days after rendezvous over the range of albedos given in Table 4 for an asteroid density of 1.6 g/cm^3.

VI. Summary and Next Steps

A demonstration mission of Ion Beam Deflection as a robust planetary defense technique is necessary to convince skeptics of the validity of the basic physics, retire known risks, and mitigate unknown unknowns. Multiple candidate near-Earth asteroids were identified that could serve as attractive targets for an IBD demonstration mission in the 2030s. This list of candidates focused on asteroids that are nominally around 50 m in diameter and are relatively easy to reach with low-thrust rendezvous trajectories. Because of the large mass uncertainty associated with asteroids with unknown albedos, it is strongly recommended that any demonstration mission be restricted to asteroids for which near-IR observations have been made. Even with a factor of 30 uncertainty in the mass, a low-cost demonstration mission to the asteroid 2004 JN1 could produce a measurable deflection after just 30 days of IBD operations. The entire duration for a demonstration mission to this asteroid would be less than one year including a 6-month cruise to the asteroid and 5 months (150 days) of post-rendezvous operations.

Next Steps. Many of the technical capabilities necessary to perform an ion-beam deflection demonstration mission have been proven in flight. In particular, there are missions that have flown low-thrust rendezvous trajectories to asteroids. Relative navigation sensors and algorithms have been demonstrated that have performed range control, feature tracking with trajectory correction maneuvers (TCMs), and asteroid centroiding. So, what challenges remain?

Proximity operations control has been exclusively managed via RCS engines. However, in order to have the benefit of high-Isp momentum exchange with the asteroid, the asteroid-relative station-keeping must be maintained with the ion engines. One could envision an approach where the ion engines are operated in open-loop fashion with throttle, gimbal angles, all computed on the ground and commanded by operators in an inner control loop with an RCS system sitting on an outer control loop controlling to the relative navigation state. However, this approach could consume a large amount of RCS propellant depending on the disturbance environment. Therefore, future work should be spent on the development and flight demonstration of an autonomous ion-engine gimbal and throttle control that closes the loop on the asteroid-relative navigation estimate. This work is ongoing at JPL.

A phase A study should be initiated with the objective to fully develop a baseline IBD demonstration mission concept, and clarify the tradeoff between human elements to achieve full system functionality and autonomous system development. The development of the technologies needed for autonomous closed-loop asteroid-relative navigation using electric thrusters should be initiated.

Finally, for actual planetary defense applications of IBD, a large, high-power gridded ion thruster with an ion beam divergence half-angle of < 5 degrees is required. The NEXIS ion thruster [8] developed for the Jupiter Icy Moons Orbiter (JIMO) mission is an excellent candidate. It has already demonstrated operation at 20 kW with a specific impulse of about 7,000 s and, when equipped with flat carbon-carbon grids, an ion beam divergence half-angle of roughly 7 degrees. This would make an excellent point of departure for the development of an IBD ion thruster for planetary defense.

Acknowledgment

The research described in this paper was carried out at the Jet Propulsion Laboratory, California Institute of Technology, under a contract with the National Aeronautics and Space Administration. Pre-decisional information — for planning and discussion purposes only.

References

1. Abell, Paul, et al., "Planetary Defense Missions, Rapid Mission Architecture Study," for the Small Solar System Bodies Planetary Science Decadal Survey, August 1, 2021.
2. Boslough, M., Brown, P., and Harris, A., "Updated Population and Risk Assessment for Airburst from Near-Earth Objects (NEOs)," IEEE Aerospace Conference, March 2015, Big Sky, MT.
3. Bombardelli C, Peláez J., "Ion beam shepherd for asteroid deflection," *Journal of Guidance Control and Dynamics*, 2011 Jul 1;34(4):1270.
4. Kitamura, S., "Large Space Debris Reorbiter Using Ion Beam Irradiation," IAC-10-A6.4.8, 61st International Astronautical Congress, September 2010.
5. Brophy, J.R., "Advanced Solar Electric Propulsion for Planetary Defense," IEPC-2015-64, Presented at Joint Conference of 30th International Symposium on Space Technology and Science, 34th International Electric Propulsion Conference and 6th Nano-satellite Symposium, Hyogo-Kobe, Japan, July 4 – 10, 2015
6. Wirz, R.E., Anderson, J.R. and Katz, I., "Time-Dependent Erosion of Ion Optics," *J. Propulsion and Power*, Vol. 27, No. 1,

January-February 2011.
7. Patterson, M.J. and Benson, S.W., “NEXT Ion Propulsion System Development Status and Capabilities, NASA/TM—2008-214988, January 2008.
8. Polk, J.E., et al., “Performance and Wear Test Results for a 20-kW-Class Ion Engine with Carbon-Carbon Grids, AIAA 2005-4393, presented at the 41st AIAA/ASME/SAE/ASEE Joint Propulsion Conference & Exhibit, 10-13 July 2005, Tucson, AZ.
9. Bombardelli C, Peláez J. Ion beam shepherd for asteroid deflection. *Journal of Guidance Control and Dynamics*, 2011 Jul 1;34(4):1270.
10. https://cneos.jpl.nasa.gov/sentry/
11. https://exoterracorp.com/products/electric-propulsion-systems/halo12-hall-thruster/
12. D. DellaGiustina et al., “Properties of rubble-pile asteroid (101955) Bennu from OSIRIS-REx imaging and thermal analysis,” *Nature Astronomy*, vol. 3, no. 4, pp. 341-351, 2019.
13. S. Lederer et al., “Physical characteristics of Hayabusa target asteroid 25143 Itokawa,” *Icarus*, vol. 173, no. 1, pp. 153-165, 2005.
14. S. Sugita et al., “The geomorphology, color, and thermal properties of Ryugu: Implications for parent-body processes,” *Science*, vol. 364, no. 6437, p. eaaw0422, 2019.
15. J. Veverka et al., “NEAR at Eros: Imaging and spectral results,” *Science*, vol. 289, no. 5487, pp. 2088-2097, 2000.
16. R. T. Daly et al., “Successful kinetic impact into an asteroid for planetary defence,” *Nature*, vol. 616, no. 7957, pp. 443-447, 2023.
17. M. Daly et al., “Hemispherical differences in the shape and topography of asteroid (101955) Bennu,” Science Advances, vol. 6, no. 41, p. eabd3649, 2020.
18. Fujiwara et al., “The rubble-pile asteroid Itokawa as observed by Hayabusa,” *Science*, vol. 312, no. 5778, pp. 1330-1334, 2006.
19. S. Watanabe et al., “Hayabusa2 arrives at the carbonaceous asteroid 162173 Ryugu—A spinning top–shaped rubble pile,” *Science*, vol. 364, no. 6437, pp. 268-272, 2019.
20. K. Berry et al., “OSIRIS-REx touch-and-go (TAG) mission design and analysis,” in 36th Annual AAS Guidance and Control Conference, 2013, no. GSFC. CP. 7566.2013.
21. G. Santo, S. C. Lee, and R. E. Gold, “NEAR spacecraft and instrumentation,” *Journal of the Astronautical Sciences*, vol. 43, no. 4, pp. 372-397, 1995.
22. E. Adams et al., “Double asteroid redirection test: The earth strikes back,” in 2019 IEEE Aerospace Conference, 2019: IEEE, pp. 1-11.
23. D. W. Dunham, J. V. McAdams, and R. W. Farquhar, “NEAR mission design,” Johns Hopkins APL technical digest, vol. 23, no. 1, pp. 18-33, 2002.
24. J. McAdams et al., “Maneuver history for the NEAR mission-Launch through Eros orbit insertion,” in Astrodynamics Specialist Conference, 2000, p. 4141.
25. G. Ono et al., “GNC strategies and flight results of Hayabusa2 first touchdown operation,”" *Acta Astronautica*, vol. 174, pp. 131-147, 2020.
26. K. Hogstrom et al., "From cocktail napkin to concept feasibility: spacecraft design in early formulation with TATER," in 2019 IEEE Aerospace Conference, 2019: IEEE, pp. 1-18.
27. Nash, "Efficient trade space exploration," in 2020 IEEE Aerospace Conference, 2020: IEEE, pp. 1-6.